

# Numerical Search for Periodic Solutions in the Vicinity of the Figure-Eight Orbit: Slaloming around Singularities on the Shape Sphere

Milovan Šuvakov

Institute of Physics Belgrade, University of Belgrade, Pregrevica 118, 11080 Beograd, Serbia

## Abstract

We present the results of a numerical search for periodic orbits with zero angular momentum in the Newtonian planar three-body problem with equal masses focused on a narrow search window bracketing the figure-eight initial conditions. We found eleven solutions that can be described as some power of the “figure-eight” solution in the sense of the topological classification method. One of these solutions, with the seventh power of the “figure-eight”, is a choreography. We show numerical evidence of its stability.

## I. INTRODUCTION

The search for periodic orbits in the three-body problem has a long history [1–10]. This work is follow-up of the previous study [11] where a systematic numerical search for periodic solutions was started and some 13 new families of solutions were reported. Here we focus on a particular window in the space of initial velocities bracketing the figure-eight initial conditions (the initial positions are fixed at the so-called Euler point). All eleven periodic solutions that we report here belong to (special) classes that can be described topologically as some power of figure-eight topological class. One of these solutions, one with the seventh power of the “figure-eight”, is a choreography.

Choreographies are a special kind of the three-body periodic orbits such that all bodies travel along the same trajectory in the plane, chasing one another around the trajectory at equal time intervals. The first and simplest choreography ever found is the Lagrange solution (1772), in which three equal-mass particles move on a circle, while forming an equilateral triangle. That solution, however, is both unstable and has non-vanishing angular momentum. The first stable three-body choreographic orbit without angular momentum was found by Moore in 1993 [12]. A formal variational existence proof for such solution is given by Chenciner and Montgomery [13].

A large number (345) of three-body choreographies with non-zero angular momentum has been found by Simó [14], but they are all highly unstable [15]. In papers [14, 16], Simó and co-authors have shown several solutions including one choreography that they called “satellites of the eight”. These satellite solutions, topologically speaking, might be associated with some power of figure-eight orbit. Here we report the discovery of one new stable, zero-angular-momentum choreographic solution to the planar Newtonian three-body problem with equal masses.

## II. DEFINITIONS AND METHODS

Before describing these solutions, we briefly remind the reader about the shape sphere coordinates that we are using for the classification of periodic solutions.

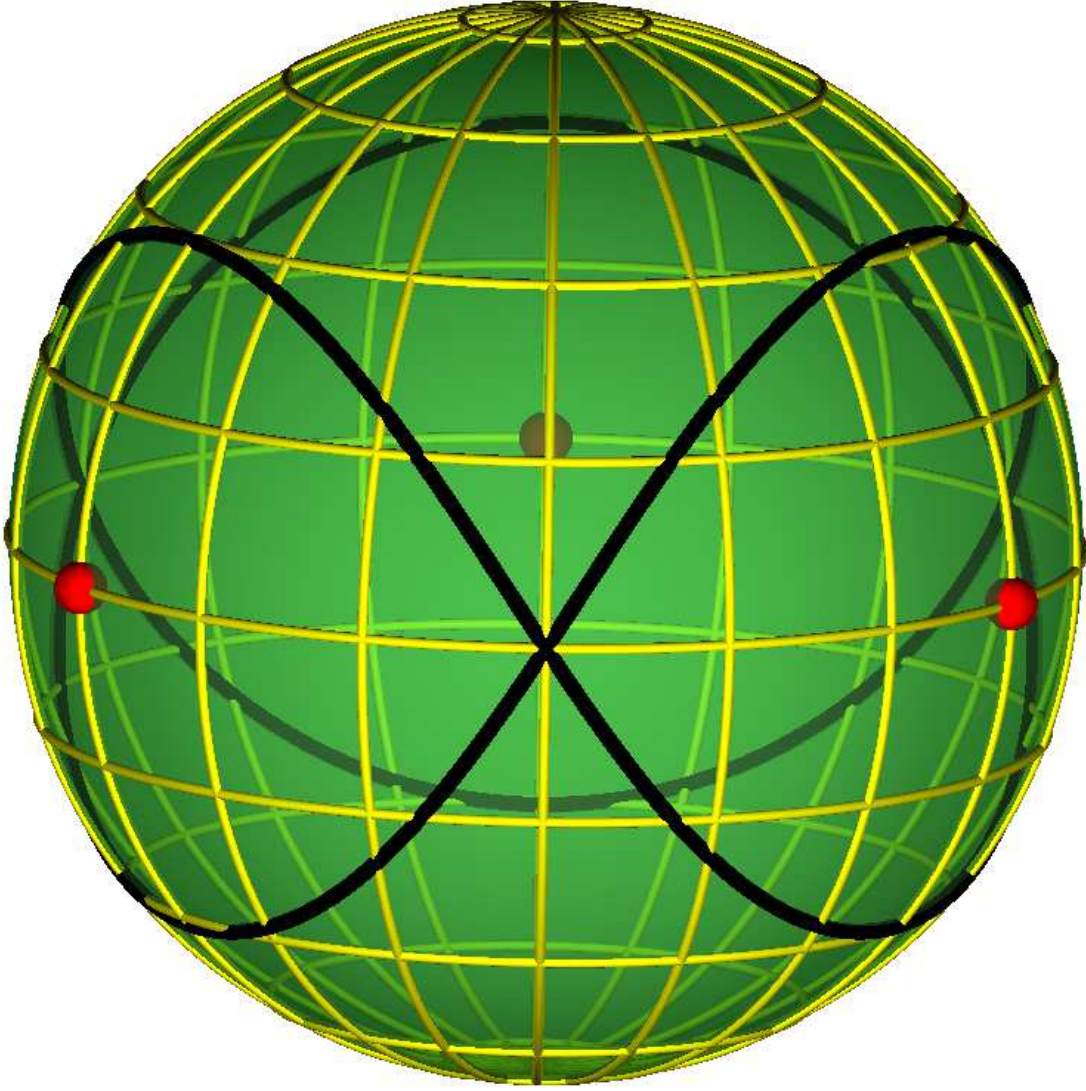


FIG. 1: Figure eight orbit (black) on the shape-space sphere. Three two-body collision points (bold red) - singularities of the potential - lie on the “equator”.

### A. Shape sphere

With two three-body Jacobi relative coordinate vectors,  $\boldsymbol{\rho} = \frac{1}{\sqrt{2}}(\mathbf{r}_1 - \mathbf{r}_2)$ ,  $\boldsymbol{\lambda} = \frac{1}{\sqrt{6}}(\mathbf{r}_1 + \mathbf{r}_2 - 2\mathbf{r}_3)$ , there are three independent scalar three-body variables. The hyper-radius  $R = \sqrt{\rho^2 + \lambda^2}$  defines the “overall size” of the system and removes one of the three linear combinations of scalar variables. Thus, one may relate the three scalars to a unit three-vector  $\hat{\mathbf{n}}$  with the Cartesian components  $\hat{\mathbf{n}} = \left( \frac{2\boldsymbol{\rho} \cdot \boldsymbol{\lambda}}{R^2}, \frac{\lambda^2 - \rho^2}{R^2}, \frac{2(\boldsymbol{\rho} \times \boldsymbol{\lambda}) \cdot \mathbf{e}_z}{R^2} \right)$ . The domain of

these three-body variables is a sphere with unit radius [17], [18], see Figure 1. The equatorial circle corresponds to collinear configurations (degenerate triangles) and the three points on it, Figure 1 correspond to two-body-collision singularities in the potential. The shape sphere together with the hyper-radius defines the configuration space of the planar three-body problem (the “missing” total rotation angle can be reconstructed from the trajectory in this space and the condition of angular momentum conservation).

The “figure-eight” solution can be described as a slalom, i.e. as moving in a zig-zag manner on the shape sphere, between the two-body singularities, while drifting in the same general direction along the equator, e.g. eastward, or westward, see Figure 1. As a consequence of parity, the number of full turns (the “winding number”) around the shape sphere sufficient to reach the initial conditions must be even, and the minimal number is two, which is the case for the figure eight orbit.

There is at least one other known solution, that makes two full turns around the shape sphere, that is stable, but not a choreography: That is Simó’s figure eight orbit (labeled by H3 in Ref. [14]). The question remains: are there any other periodic orbits with a higher winding number? Such an orbit would have to “miss” the initial point in the phase space at each turn before the last one. Again, due parity, the winding number of such a trajectory has to be an even number  $2k$ ,  $k \in \mathbb{N}$ . If there are such solutions, then another question is: are there any choreographies among them?

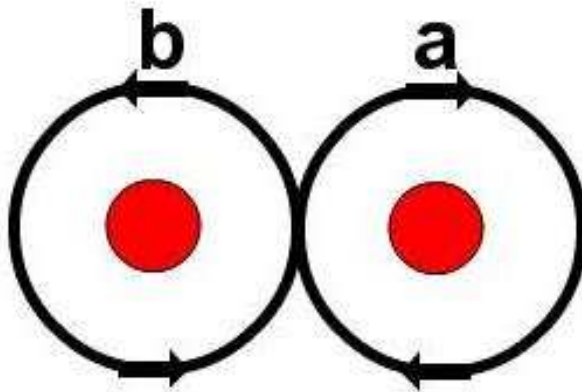


FIG. 2: Diagrammatic representation of the two free group elements.

## B. Topological classification

We use the topological classification of periodic three-body solutions, suggested by Montgomery [19]. Considering a periodic orbit as a closed curve on a sphere with three punctures (the shape sphere with three singularities of the potential), the classification of closed curves is given by the conjugacy classes of the fundamental group, which is, in this case, the free group on two letters  $(a, b)$ .

Graphically, this amounts to classifying closed curves according to their “topologies” on a sphere with three punctures. A stereographic projection of this sphere onto a plane, using one of the punctures as the “north pole” effectively removes that puncture to infinity, and reduces the problem to one of classifying closed curves in a plane with two punctures. That leads to the aforementioned free group on two letters  $(a, b)$ , where (for definiteness)  $a$  denotes a clockwise “full turn/circle” around the right-hand-side puncture, and  $b$  denotes the counter-clockwise full turn/circle around the other pole/hole/puncture in the plane/sphere, see Fig. 2.

For better legibility we denote their inverses by capitalized letters  $a^{-1} = A, b^{-1} = B$ . Each family of orbits is associated with the conjugacy class of a free group element. For example the conjugacy class of  $aB$  contains  $A(aB)a = Ba$ . The “figure-eight” orbit is related to the conjugacy class of the element  $abAB$ . The aforementioned curves with a “winding number”  $2k$  belong to the conjugacy class of the group element  $(abAB)^k$ . Orbits of this kind will be called **slaloms** and the exponent  $k$  will be called the **slalom power**.

## C. Search strategy

Here we use the same numerical approach as in Ref. [11]. The return proximity function in the phase space is defined as the absolute minimum of the distance from the initial condition by

$$d(\mathbf{X}_0, T_0) = \min_{t \leq T_0} |\mathbf{X}(t) - \mathbf{X}_0|, \quad (1)$$

where  $\mathbf{X}(t) = (\mathbf{r}_1(t), \mathbf{r}_2(t), \mathbf{r}_3(t), \mathbf{p}_1(t), \mathbf{p}_2(t), \mathbf{p}_3(t))$  is a 12-vector in the phase space (all three bodies’ Cartesian coordinates and velocities, i.e. without removing the center-of-mass motion), and  $\mathbf{X}_0 = \mathbf{X}(0)$  is 12-vector describing the initial condition. We also define the return time  $\tau(\mathbf{X}_0, T_0)$  as the time for which this minimum is reached. Searching for periodic

solutions with a period  $T$  smaller than the parameter  $T_0$  is clearly equivalent to finding zeros of the return proximity function.

The initial conditions for both Moore’s [12] and Simó’s [14] figure eight solutions can be found in the two dimensional subspace of the eight-dimensional three-body phase space with the center-of-mass motion removed, see Fig. 3. Formally this two dimensional search plane is defined as the set of collinear configurations (“syzygies”) with one body exactly in the middle between the other two (the so-called Euler points), and with vanishing initial time derivative of the hyper-radius  $\dot{R} = 0$  and vanishing angular momentum. In this subspace, all three particles’ initial conditions can be specified by two parameters, the initial  $x$  and  $y$  components,  $\dot{x}_1(0)$  and  $\dot{y}_1(0)$ , respectively, of a single velocity two-vector, as follows,  $x_1(0) = -x_2(0) = -1$ ,  $x_3(0) = 0$ ,  $y_1(0) = y_2(0) = y_3(0) = 0$ ,  $\dot{x}_2(0) = \dot{x}_1(0)$ ,  $\dot{x}_3(0) = -2\dot{x}_1(0)$ ,  $\dot{y}_2(0) = \dot{y}_1(0)$ ,  $\dot{y}_3(0) = -2\dot{y}_1(0)$ .

The differential equations of motion were solved numerically using the Runge-Kutta-Fehlberg 4.5 method and the return proximity function was calculated using linear interpolation between calculated trajectory points in the phase space. In all our calculations, the particle masses  $m_1$ ,  $m_2$ ,  $m_3$  and Newton’s gravitational constant  $G$  were set equal to unity.

### III. RESULTS

We focused our numerical search on the (two-dimensional) search window in the two dimensional search plane (defined above) around the “figure-eight” initial conditions:  $\dot{x}_1(0) \in (0.20, 0.46)$ ,  $\dot{y}_1(0) \in (0.51, 0.56)$ , see Figure 3. The equations of motion were integrated up to time  $T_0 = 100$  for each initial condition out of  $130 \times 1000$  possibilities (points on the grid) within the search window. The return proximity function  $d(\mathbf{X}_0, T_0)$  was calculated and is shown in Figure 3. For each local minimum of the return proximity function lower than  $10^{-4}$  (bright dots in Figure 3) on this grid we used the simple gradient descent algorithm to find the position of the minimum (root) more accurately. All minima below  $10^{-6}$  are listed in Table I and can be seen in Figure 3. The initial conditions for Moore’s “figure-eight” choreography and Simó’s “figure-eight” orbit are labeled by  $M8$  and  $S8$ , respectively in Table I. All other labeled orbits in Table I are slaloms of power  $k$ .

There is a restriction on the slalom power  $k$  in the case of choreographic solutions. If a solution is a choreography, the three masses follow each other, with a time delay of  $T/3$ ,

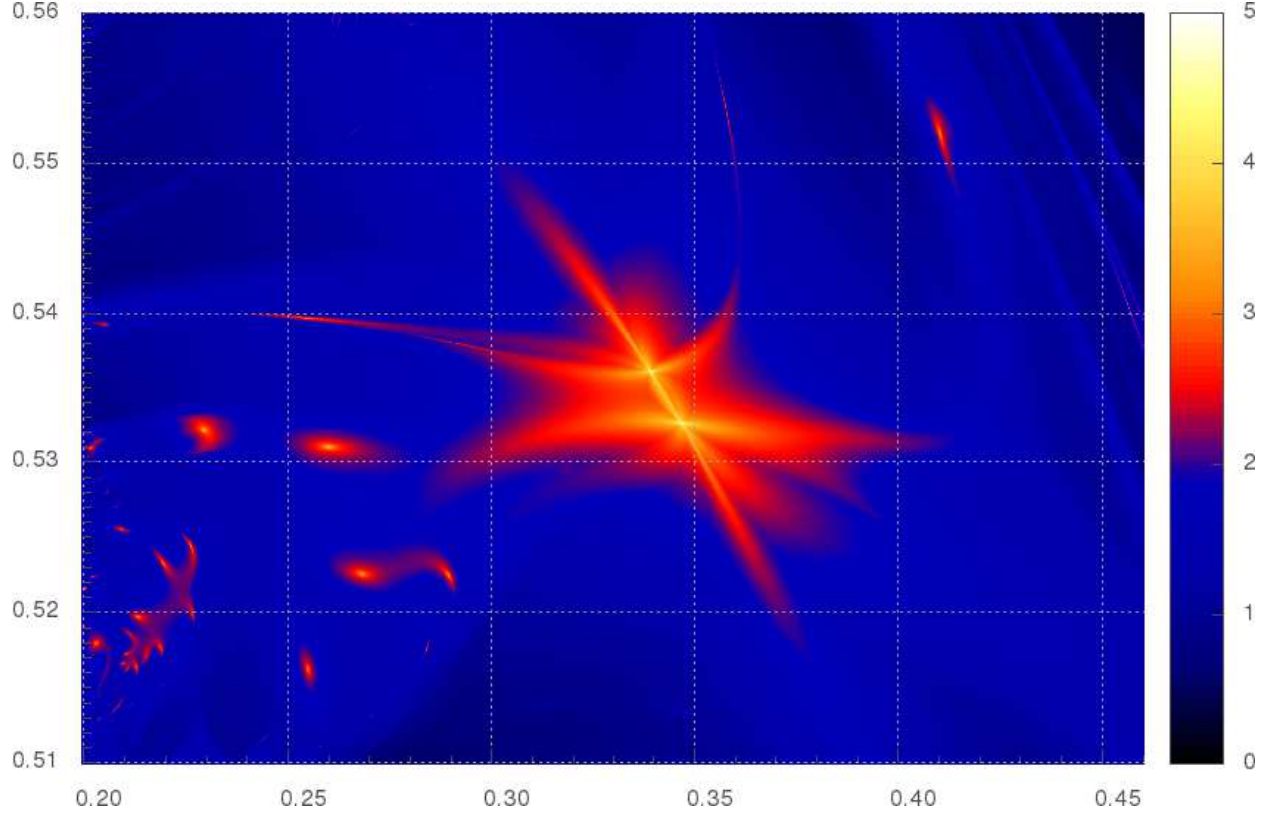


FIG. 3: The decimal logarithm of the reciprocal of the return proximity function  $-\log_{10} d(\mathbf{X}_0, T_0)$  in the search window around the initial conditions for the figure-eight solutions in search plane. On x-axis are the values of the initial velocity  $\dot{x}_1(0) \in (0.20, 0.46)$ , and on the y-axis are the values of the initial velocity  $\dot{y}_1(0) \in (0.51, 0.56)$ .

where  $T$  is the full period. If one follows a choreography starting with a delay of  $T/3$ , one sees the same motion as without that delay, up to a cyclic permutation of three particles [21]. Algebraically, this can be written as  $\mathbf{X}(t + T/3) = \hat{P}\mathbf{X}(t)$ , where  $\hat{P}$  is a cyclic permutation. The cyclic permutation  $\hat{P}$  has a simple representation on the shape sphere, *viz.* a rotation by  $2\pi/3$  around the vertical z-axis. For a choreography the azimuthal angle on the shape sphere after motion through time  $T/3$  will be  $2\pi k/3$ . Therefore, the slalom power  $k$  of any choreography can not be a number divisible by 3 (otherwise  $2\pi k/3$  is an integer multiple of  $2\pi$ , and the net rotation mustnot be  $2\pi/3$ ).

TABLE I: Initial conditions and periods of three-body orbits.  $\dot{x}_1(0), \dot{y}_1(0)$  are the first particle's initial velocities in the x- and y-directions, respectively,  $T$  is the period,  $k$  is slalom power (i.e.  $abAB^k$  is homotopy class of the orbit), and the last column is the geometric-algebraic (g-a) class (for explanation see text). We also list Moore's ( $M8$ ) and Simó's ( $S8$ ) figure-eight orbits, for comparison.

Label	$\dot{x}_1(0)$	$\dot{y}_1(0)$	T	$k$	g-a class
$M8$	0.3471128135672417	0.532726851767674	6.3250	1	I.A
$S8$	0.3393928985595663	0.536191205596924	6.2917	1	I.A
$NC1$	0.2554309326049807	0.516385834327506	35.042	7	II.A
$NC2$	0.4103549868164067	0.551985438720704	57.544	7	II.A
$O1$	0.2034916865234370	0.5181128588867190	32.850	7	IV.A
$O2$	0.4568108129224680	0.5403305086130216	64.834	7	IV.A
$O3$	0.2022171409759519	0.5311040339355467	53.621	11	IV.A
$O4$	0.2712627822083244	0.5132559436920279	55.915	11	IV.A
$O5$	0.2300043496704103	0.5323028446350102	71.011	14	IV.A
$O6$	0.2108318037109371	0.5174100244140625	80.323	17	IV.A
$O7$	0.2132731670875545	0.5165434524230961	80.356	17	IV.A
$O8$	0.2138543002929687	0.5198665707397461	81.217	17	III.A
$O9$	0.2193730914764402	0.5177814195442197	81.271	17	III.A
$O10$	0.2272123532714848	0.5200484344272606	82.671	17	IV.A
$O11$	0.2199766127929685	0.5234338500976567	82.743	17	IV.A
$O12$	0.2266987607727048	0.5246235168190009	83.786	17	III.A
$O13$	0.2686383642458915	0.5227270888731481	88.674	17	III.A
$O14$	0.2605047016601568	0.5311685141601564	89.941	17	IV.A
$O15$	0.2899041109619139	0.5226240653076171	91.982	17	IV.A

### A. The $k = 7$ choreography

All solutions listed in Table I satisfy the above choreography condition, but only solutions labeled  $NC1$  and  $NC2$  are choreographies. It turns out that these two solutions



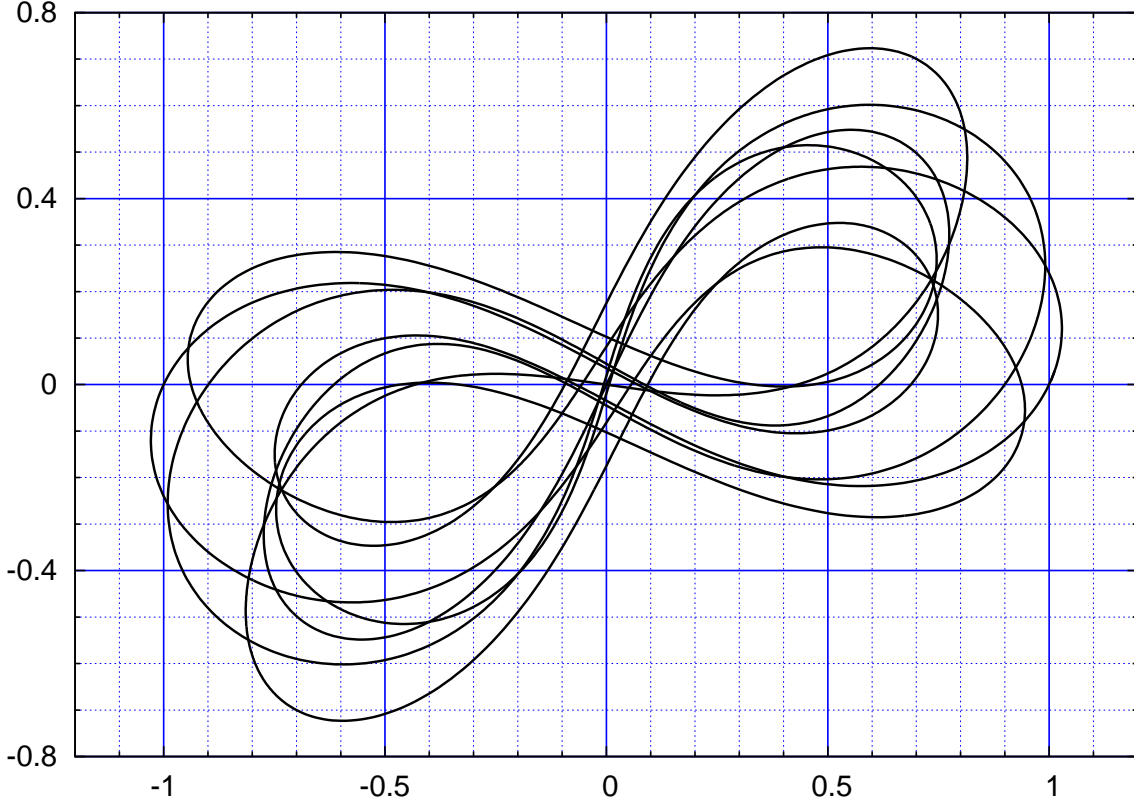


FIG. 4: The trajectory of the new choreography in the (real)  $x$ - $y$  plane.

are equivalent, up to rescaling of temporal and spatial coordinates by the scaling law [20]:  $\mathbf{r} \rightarrow \alpha \mathbf{r}$ ,  $t \rightarrow \alpha^{3/2} t$ , and consequently  $\mathbf{v} \rightarrow \mathbf{v}/\sqrt{\alpha}$ . The trajectory  $HC1$  in real space is shown in Figure 4. This solution is centrally symmetric with respect to reflections about the origin, which is the initial position of the “middle” mass, as a consequence of the fact that all bodies follow the same trajectory, that equations of motion are symmetric under time reversal and that all initial conditions are symmetric under the combined action of parity  $\mathcal{P}$ , time-reversal  $\mathcal{T}$  and transposition  $P_{12}$ . It appears that our choreography does not have any additional symmetries in real space. The slalom power  $k$  of this solution is seven.

The trajectory in real space is composed of seven concatenated distorted figure-eight curves, Fig. 4. The trajectory passes through the coordinate origin twice. By following the position of the second mass one can see that the first passage through the origin corresponds to the initial time, whereas the second one corresponds to the point in time when the phase space position scales into the  $NC2$  initial condition. The curves  $HC1$  and  $HC2$  in the  $x-y$  plane are connected by a homothetic transformation with a homothety factor  $\lambda \approx -1.3919$

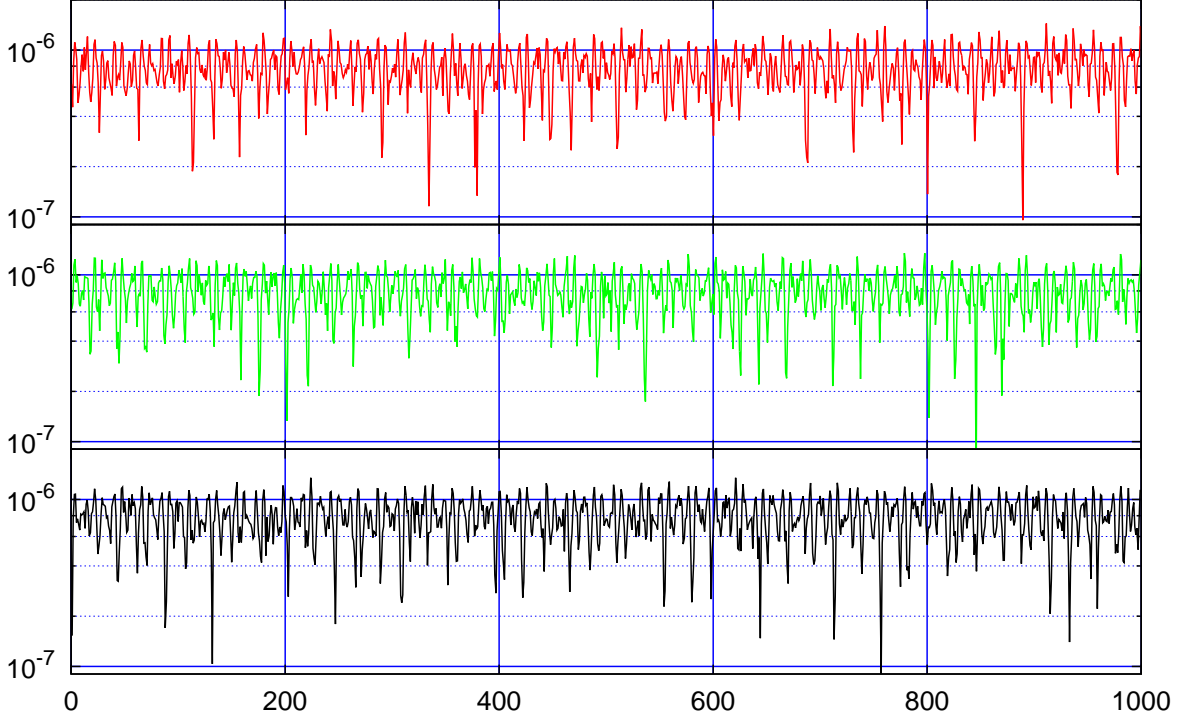


FIG. 5: The minimal distance between initial condition and trajectory per each period  $D_{0i}^T$  (bottom panel); and the minimal distance between initial conditions and two cyclic permutations of the phase space coordinates:  $D_{1i}^T$  and  $D_{2i}^T$  (middle and top panel).

and rotation angle of  $\approx 0.252\pi$  radians. The minus sign in the homothety factor  $\lambda$  means that the two trajectories have opposite orientations, or in physical terms, that these two motions are time reversed.

The key feature of this choreography is its stability. The return proximity per period:  $D_{0i}^T = \min_{iT \leq t < (i+1)T} |\mathbf{X}(t) - \mathbf{X}_0|$ , where  $T$  is period, is calculated up to a thousand periods (i.e. 42000 syzigies) and is shown in Fig 5. In order to check if this solution is a true choreography, we show on the same plot:  $D_{1i}^T = \min_{iT \leq t < (i+1)T} |\hat{P}\mathbf{X}(t) - \mathbf{X}_0|$ , and  $D_{2i}^T = \min_{iT \leq t < (i+1)T} |\hat{P}^2\mathbf{X}(t) - \mathbf{X}_0|$ , the minimal distances per period between the initial condition point and the two cyclic permutations of the trajectory coordinates in the phase space, respectively. Whereas the first array is zero for any periodic solution, all three arrays are zero when the solution is a choreography. One can see in Figure 5 that all three values fluctuate around an approximately constant level of  $10^{-6}$ . Running our calculation up to 25,000 periods (or one million syzigies) we see that the noise level slowly rises in time, reaching the value  $5 \cdot 10^{-6}$  towards the end of our computation. This is comparable with

the cumulative numerical error in this calculation.

### B. The $k = 7, 11, 14$ slaloms

Other solutions (denoted by  $O\#$ ) shown in Table I correspond to different slalom powers  $k$ . The first one, denoted by  $O1$ , belongs to the same slalom power  $k = 7$  as the new choreography solution, but it is not a choreography. The second one  $O2$  is the same solution as the first one  $O1$ , up to a rotation and scaling of space-time. The two slalom power  $k = 11$  solutions  $O3$  and  $O4$  are also identical. The solution  $O5$  has slalom power  $k = 14$ .

### C. Scaling of $k = 17$ slaloms

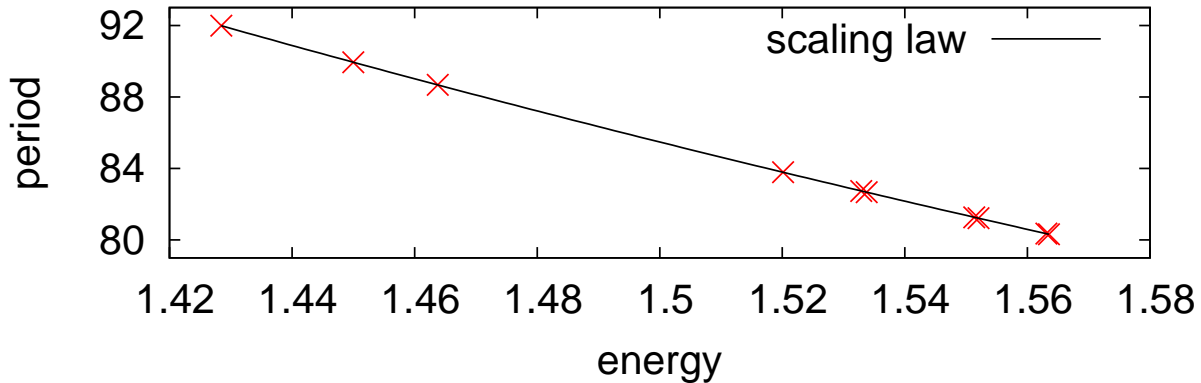


FIG. 6: Red crosses: period  $T$  vs. absolute value of energy  $\varepsilon$  for slalom orbits with power  $k = 17$ . Solid line: fit according to the scaling law  $T \sim \varepsilon^{-3/2}$  (for details, see text).

All other solutions ( $O6$ - $O15$ ) have the slalom power  $k = 17$ , but demand special attention to determine if they are identical. In Figure 6 we show the period  $T$  as a function of the absolute value of the energy  $\varepsilon = |E|$  for these orbits. The fitting parameter  $A$  for the fit shown in Figure 6 with the scaling law  $T = A\varepsilon^{-3/2}$  is:  $A = 157.036 \pm 0.0007235$ , with the reduced  $\chi$ -square value of  $\chi_{red}^2 = 1.51197 \times 10^{-6}$ . Such good agreement with the scaling law indicates that all these solutions may correspond to the same orbit.

A careful analysis of passages through Euler points shows, however, that there are seven different  $k = 17$  slaloms. Solutions  $O6$  and  $O7$  correspond to same orbit. This is also the case with  $O10$  and  $O11$ , and with  $O14$  and  $O15$ . On the shape sphere each of these pairs of

solutions has exactly the same trajectory, whereas their real-space trajectories are related by scaling transformations.

#### D. Geometric-algebraic classification of results

All solutions presented here fall into three new algebraic-geometric classes according to the classification scheme defined in Ref. [11]. There were two different geometric classes defined in [11]: (I) those with (two) reflection symmetries about two orthogonal axes — the equator and the zeroth meridian passing through the "far" collision point; and (II) those with a (single) central reflection symmetry about one point — the intersection of the equator and the aforementioned zeroth meridian. Here, we have found two additional classes: (III) those with reflection symmetries about only one axis — the equator; and (IV) those without any geometric symmetry on the shape sphere.

Similarly, in Ref. [11] orbits were divided according to the algebraic exchange symmetries of (conjugacy classes of) their free group elements: (A) with free group elements that are symmetric under  $a \leftrightarrow A$  and  $b \leftrightarrow B$ , (B) with free group elements symmetric under  $a \leftrightarrow b$  and  $A \leftrightarrow B$ , and (C) with free group elements that are not symmetric under either of the two symmetries (A) or (B).

We have observed empirically in Ref. [11] that, for all orbits presented there, the algebraic symmetry class (A) corresponds to the geometric class (I), and that the algebraic class (C) corresponds to the geometric class (II), whereas the algebraic class (B) may fall into either of the two geometric classes.

However, our new choreography solution does not obey this rule. It belongs to the algebraic symmetry class (A), but corresponds to the geometric class (II). This defines a new geometric-algebraic class II.A. The remaining solutions (slaloms) presented here define two additional classes: III.A and IV.A (see the last column in table I).

## IV. CONCLUSIONS

In conclusion, as the result of numerical studies, we have found 11 new three-body solutions that can be described as slaloms with powers  $k = 7, 11, 14, 17$ . One of these solutions ( $NC1 = NC2$ ), with  $k = 7$ , is a stable choreography. This particular orbit ought to be of

special interest to mathematicians interested in rigorous existence proofs of three-body solutions. Other new non-choreographic orbits hold the same general interest as the solutions found in Ref. [11].

## Acknowledgments

The author would like to thank V. Dmitrašinović for his help in the early stages of this work and with the write-up of this paper, and to Prof. Carles Simó for providing information about his solutions. This work was supported by the Serbian Ministry of Education, Science and Technological Development under grant numbers OI 171037 and III 41011. The computing cluster Zefram (zefram.ipb.ac.rs) has been extensively used for calculations.

- 
- [1] H. Poincaré, chapter XXIX, no 341, in *Les méthodes nouvelles de la mécanique céleste*, tomes I (1892) & III (1899), Réédition Blanchard, Paris (1987), (in French, the sentence translated by A. Chenciner).
  - [2] R. Broucke and D. Boggs, *Celest. Mech.* **11**, 13 (1975).
  - [3] J.D. Hadjidemetriou, *Celest. Mech.* **12**, 155 (1975).
  - [4] J.D. Hadjidemetriou and Th. Christides, *Celest. Mech.* **12**, 175 (1975).
  - [5] J.D. Hadjidemetriou, *Celest. Mech.* **12**, 255 (1975).
  - [6] R. Broucke, *Celest. Mech.* **12**, 439 (1975).
  - [7] M. Henon, *Celest. Mech.* **13**, 267 (1976).
  - [8] M. Henon, *Celest. Mech.* **15**, 243 (1977).
  - [9] R. Vanderbei, *Ann. N.Y. Acad. Sci.* **1017**, 422 (2004).
  - [10] V.B. Titov, *Nelin. Dinam.* **8** 2 (2012) 377389
  - [11] M. Šuvakov and V. Dmitrašinović, *Physical Review Letters* **110** (11), 114301 (2013)
  - [12] C. Moore, *Phys. Rev. Lett.* **70**, 3675 (1993).
  - [13] A. Chenciner and R. Montgomery, *Annals of Mathematics*, **152** 3 (2000) 881-901
  - [14] C. Simó, *Contemp Math* **292** 20928 (2002).
  - [15] C. Simó (private communication, 2012).

- [16] A. Chenciner, J. Gerver, R. Montgomery, C. Simó *Geometry, Mechanics, and Dynamics*, Springer 2002, pp 287-308
- [17] T. Iwai, *J. Math. Phys.* **28**, 964, 1315 (1987).
- [18] R. Montgomery, *Nonlinearity* **9** 1341 (1996). doi:10.1088/0951-7715/9/5/014
- [19] R. Montgomery, *Nonlinearity* **11**, 363 - 376 (1998).
- [20] L. D. Landau and E. M. Lifshitz, *Mechanics*, 3rd ed. (Butterworth-Heinemann, Oxford, 1976), Sec. 10.
- [21] where the first mass is substituted into the position of the second, the second into the third, and the third into the position of the first.